Cell, Vol. 110, 725–735, September 20, 2002, Copyright ©2002 by Cell Press

Modulation of Cardiac Growth and Development by HOP, an Unusual Homeodomain Protein

Chong Hyun Shin,[1,6] Zhi-Ping Liu,[1,6] Robert Passier,[1,4,6] Chun-Li Zhang,[1] Da-Zhi Wang,[1] Thomas M. Harris,[3] Hiroyuki Yamagishi,[1] James A. Richardson,[2] Geoffrey Childs,[3] and Eric N. Olson[1,5]

[1]Department of Molecular Biology
[2]Department of Pathology
University of Texas Southwestern Medical Center at Dallas
6000 Harry Hines Boulevard
Dallas, Texas 75390
[3]Department of Molecular Genetics
Albert Einstein College of Medicine
1300 Morris Park Avenue
Bronx, New York 10461
[4]Hubrecht Laboratory
Uppsalalaan 8
3584CT Utrecht
The Netherlands

Summary

We have discovered an unusual homeodomain protein, called HOP, which is comprised simply of a homeodomain. HOP is highly expressed in the developing heart where its expression is dependent on the cardiac-restricted homeodomain protein Nkx2.5. HOP does not bind DNA and acts as an antagonist of serum response factor (SRF), which regulates the opposing processes of proliferation and myogenesis. Mice homozygous for a *HOP* null allele segregate into two phenotypic classes characterized by an excess or deficiency of cardiac myocytes. We propose that HOP modulates SRF activity during heart development; its absence results in an imbalance between cardiomyocyte proliferation and differentiation with consequent abnormalities in cardiac morphogenesis.

Introduction

Organ formation during embryogenesis requires the commitment of multipotent progenitor cells to specific lineages, the activation of tissue-specific genes, and the precise spatial organization of specialized cell types. A tightly regulated balance between cell proliferation and differentiation is also required to generate and maintain the size and shape of the mature organ. These processes are controlled by combinatorial interactions between cell-specific and broadly expressed transcription factors that act through positive and negative mechanisms to govern arrays of target genes in distinct temporospatial patterns.

Members of the homeodomain family of transcription factors play key roles in organogenesis and embryonic patterning by interpreting positional information in the embryo and linking extracellular signals to tissue-specific gene regulatory programs (reviewed in Gehring et al., 1994). The homeodomain is encoded by a DNA sequence referred to as the homeobox. Homeobox genes are found in all eukaryotic organisms, and over 160 have potentially been identified in the human genome. Homeodomain proteins can be categorized into different classes based on amino acid sequence homologies within the homeodomain and their expression patterns. A subset of homeobox genes located in clusters confers positional information along the antero-posterior axis of the embryo. Numerous other homeobox genes are distributed throughout the genome and show unique expression patterns.

The homeodomain is comprised of 60 amino acids that adopt three α helices, with a characteristic helix-turn-helix motif (reviewed in Kornberg, 1993). Helix-3, referred to as the recognition helix, lies in the major groove of the DNA binding site and makes direct contact with the DNA. Amino acid variations within the recognition helix dictate DNA binding site specificity of different homeodomain proteins. Additional specificity of DNA binding is contributed by a flexible region, called the N-terminal arm, that extends from the first helix and wraps around the DNA to make contacts with the minor groove.

Target gene specificity of different homeodomain proteins that bind the same DNA sequence is achieved through differential association with positive and negative cofactors. Such interactions can occur between homeodomain proteins and other transcriptional regulators that bind adjacent sequences in regulatory DNA or by direct protein-protein interactions in the absence of DNA binding. A classic example of such combinatorial interactions is illustrated by the yeast homeodomain protein MATα2, which interacts with the MADS (MCM1, Agamous, Deficiens, and serum response factor) box transcription factor MCM1, resulting in repression of a-specific genes (Smith and Johnson, 1992). Similarly, homeodomains of the Paired-type associate with serum response factor (SRF), a MADS box factor that controls the expression of genes involved in cell proliferation and myogenesis (Norman et al., 1988; Reecy et al., 1998). Association of SRF with the phox/prx1 homeodomain protein enhances the binding of SRF to DNA (Grueneberg et al., 1992). The association of MADS box proteins like MCM1 and SRF with homeodomain proteins couples cell identity with signal responsiveness, thereby providing a mechanism for cell type-specific responses to "generic" signals.

The cardiac-restricted homeodomain protein, Nkx2.5, also associates with SRF, resulting in cooperative activation of cardiac genes (Chen and Schwartz, 1996; Sepulveda et al., 2002). *Nkx2.5*, which is among the earliest markers of heart formation in vertebrate embryos (Lints et al., 1993), is an ortholog of *tinman*, a homeobox gene required for heart formation in *Drosophila* (reviewed in Harvey, 1996). *Nkx2.5* is expressed throughout the developing and adult heart (Lints et al., 1993). Mice homozygous for an *Nkx2.5* null allele die during embryogenesis

[5]Correspondence: eolson@hamon.swmed.edu
[6]These authors contributed equally to this work.

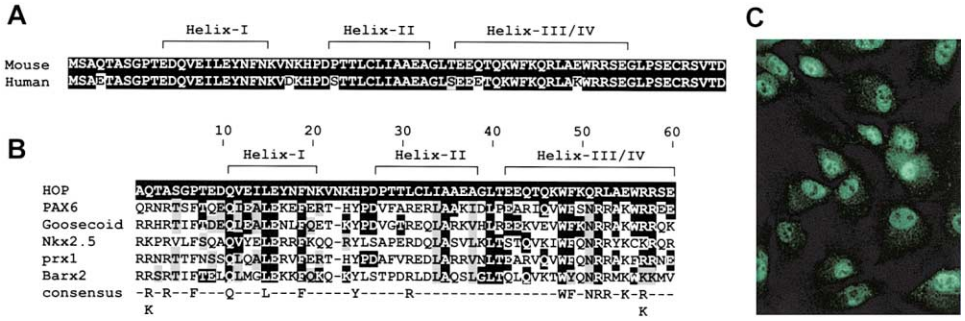

Figure 1. Sequence Comparison of HOP and Other Homeodomain Proteins

(A) Alignment of the deduced amino acid sequences of mouse and human HOP proteins.

(B) Sequence comparison of the homeodomain of mouse HOP with other homeodomains. Amino acid positions within the 60 amino acid homeodomain are shown.

(C) Localization of HOP protein to the nucleus in primary rat cardiomyocytes. Myocytes were stained with anti-HOP antibody.

from myogenic and morphologic cardiac abnormalities (Lyons et al., 1995; Tanaka et al., 1999).

Here we describe an unusual homeodomain protein, called Homeodomain-Only Protein (HOP), which is expressed in the developing heart where it is regulated by Nkx2.5. We originally named this protein Cameo (cardiac homeodomain) and Epstein and coworkers, who discovered it independently, named it Toto (Chen et al., 2002 [this issue of *Cell*]). Through the generation of mice lacking HOP, we show that HOP acts at multiple steps in the pathway for heart development.

Results

Structure of the HOP Homeodomain

We performed a bioinformatics screen of expressed sequence tag (EST) databases using a homeodomain consensus sequence to identify unknown homeobox genes expressed in the developing heart. One potential homeobox sequence we identified and subsequently cloned from a mouse heart cDNA library appeared to encode an unusually small 73 amino acid homeodomain protein, which we named Homeodomain-Only Protein (HOP; Figure 1A). There were multiple in-frame termination codons upstream of the initiating methionine in the HOP cDNA sequences, indicating that this is the complete open reading frame. The predicted mouse HOP protein has a Mr = 8.3 kDa and a pI of 4.64. Mouse and rat cDNA sequences encoding identical HOP proteins and a human sequence with six amino acid differences were identified (Figure 1A). We did not identify a HOP-like sequence in *Drosophila* or *Caenorhabditis elegans* genome sequences, suggesting that this gene may be specific to vertebrates.

HOP is an unusually small homeodomain protein. Secondary structural predictions indicate that HOP forms three α helices with a helix-turn-helix motif characteristic of the homeodomain. The HOP homeodomain contains numerous residues that are highly conserved throughout the homeodomain superfamily (Figure 1B). The WF motif at residues 48 and 49 of the homeodomain is conserved in almost all homeodomain proteins and partially defines this class of transcription factors. Residue 50 within the recognition helix controls the specificity of DNA binding by determining base preferences and is a signature residue for different types of homeodomains. The lysine at this position in HOP is characteristic of the paired-type homeodomain subclass, which includes Pax-6 and goosecoid. Glutamine-11, leucine-15, phenylalanine-19, alanine-35, leucine-40, and arginines-52 and -57 are also highly conserved in other homeodomains and are present in HOP.

There are also several divergent amino acids within the HOP homeodomain, some of which would be predicted to be incompatible with efficient DNA binding. For example, the nine amino acids immediately preceding helix-1 of other homeodomains contain highly conserved basic residues that extend across the DNA binding site and make contact with the DNA minor groove. There are no basic residues in this region of HOP and there is a Gly-Pro sequence that would alter the structure of this amino-terminal arm. HOP contains a glutamine at position 51, whereas every other metazoan homeodomain contains an asparagine at this position, which makes identical base-specific contacts with a conserved adenine in the binding sites of all homeodomain structures that have been determined (Kornberg, 1993). Residues 53 and 55 are also almost always arginine and lysine, respectively, in other homeodomains, whereas in HOP these residues are leucine and glutamic acid. Since these residues of other homeodomains make direct contact with the DNA through electrostatic interaction, the presence of hydrophobic and negatively charged residues at these positions is unfavorable for DNA binding.

We tested whether a bacterial GST-HOP fusion protein was able to bind DNA by performing gel mobility shift assays with binding sites for other homeodomain proteins and by PCR-mediated binding site selection assays with random oligonucleotide probes. No DNA binding of HOP was observed. Nevertheless, immunostaining of isolated rat cardiomyocytes with an anti-HOP antibody showed that HOP protein was localized predominantly to the nucleus (Figure 1C).

Expression of HOP

During mouse embryogenesis, *HOP* transcripts were first detected at E7.75 in trophoblasts within extraem-

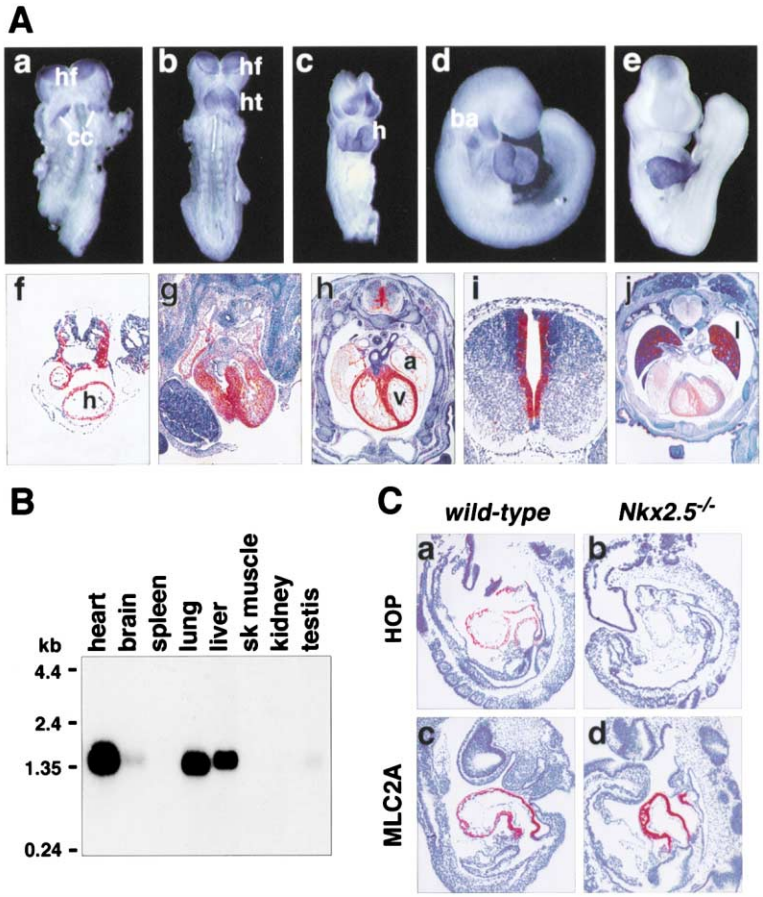

Figure 2. Expression Pattern of HOP during Mouse Embryogenesis and in Adult Mouse Tissues

(A) In (a–e), HOP transcripts were detected by whole-mount in situ hybridization to mouse embryos at (a) E7.75, (b) E8.0, (c) E8.5, (d) E9.5, and (e) E11.5. In (f–j), HOP transcripts were detected by in situ hybridization to transverse sections as follows: (f) staining in lateral mesoderm and heart tube at E8.5, (g) staining throughout the atrial and ventricular chambers at E12.5, (h) staining in heart and neural tube at E14.5, (i) high magnification of neural tube at E12.5, and (j) staining in heart and lungs at E16.5. a, atrium; ba, branchial arch; cc, cardiac crescent; h, heart; hf, head fold; ht, heart tube; l, lung; v, ventricle.

(B) Detection of HOP mRNA by Northern blot of adult mouse tissues. Equal amounts of RNA were loaded in each lane.

(C) In situ hybridization of sagittal sections of wild-type and *Nkx2.5*$^{-/-}$ embryos, as indicated. HOP transcripts are not detected in the heart of the *Nkx2.5*$^{-/-}$ mutant. MLC2A transcripts are detected in embryos of both genotypes, confirming integrity of mRNA in the mutant.

bryonic membranes (data not shown). At E7.75, *HOP* transcripts were detected in the lateral wings of the cardiac crescent and in the anterior head folds (Figure 2A, a). Expression of *HOP* in the cardiac crescent lags behind that of *Nkx2.5* by about 8 hr and is less extensive; whereas *Nkx2.5* is expressed throughout the cardiac crescent (Lints et al., 1993), *HOP* expression is restricted to the lateral domains. At E8.0, *HOP* expression was detected along the length of the linear heart tube and in the head folds (Figure 2A, b). At E8.5 to 9.5, expression was also observed in the branchial arches and lateral mesoderm dorsal to the heart (Figure 2A, c, d, and f). Expression was maintained throughout the ventricular and atrial chambers of the heart through E14.5 (Figure 2A, e, g, and h). Beginning at about E12.5, we also observed *HOP* expression within the periventricular zone of the neural tube, and by E16.5, expression of *HOP* was observed in the epithelium of the developing airways of the lungs (Figure 2A, i and j). A single *HOP* transcript of 1.3 kb was detected in adult mouse heart, lung, brain, and liver (Figure 2B).

Dependence of *HOP* Expression on *Nkx2.5*

To begin to determine whether *HOP* might act within the network of genes that controls heart formation, we examined its expression in a series of mouse mutants with abnormalities in specific steps of cardiac development. Cardiac expression of *HOP* was downregulated in *Nkx2.5* mutant embryos (Figure 2C), which fail to form a left ventricular chamber (Lyons et al., 1995). *HOP* was expressed at normal levels in mice lacking the bHLH transcription dHAND, which fail to form a right ventricle (Srivastava et al., 1997), or MEF2C, which show abnormal atrial and ventricular development (Lin et al., 1997; data not shown). We conclude that *HOP* expression is dependent on Nkx2.5 during the early stages of heart development.

Generation of *HOP* Mutant Mice

To investigate the function of *HOP* in vivo, we generated *HOP* null mice by gene targeting (Figures 3A and 3B). Our targeting vector deleted the entire coding region and introduced a nuclear-localized lacZ protein-coding region in-frame with the initiation codon of *HOP*.

Mice heterozygous for the *HOP* null mutation were intercrossed to obtain *HOP* null offspring in the isogenic 129Sv background, as well as in the 129Sv/C57BL6 mixed background. In the mixed genetic background, viable homozygous mutants were obtained at postnatal day 10 (P10) at a frequency that approximated Mendelian ratios (Table 1). However, in the isogenic 129Sv background, viable homozygous mutants were underrepresented at a frequency of 17% compared to the predicted 25% (Table 1). These findings suggested that the *HOP* mutant phenotype resulted in embryonic lethality with variable penetrance.

Northern blot and RT-PCR analysis of RNA from heart and liver of *HOP* null mice confirmed that the targeted

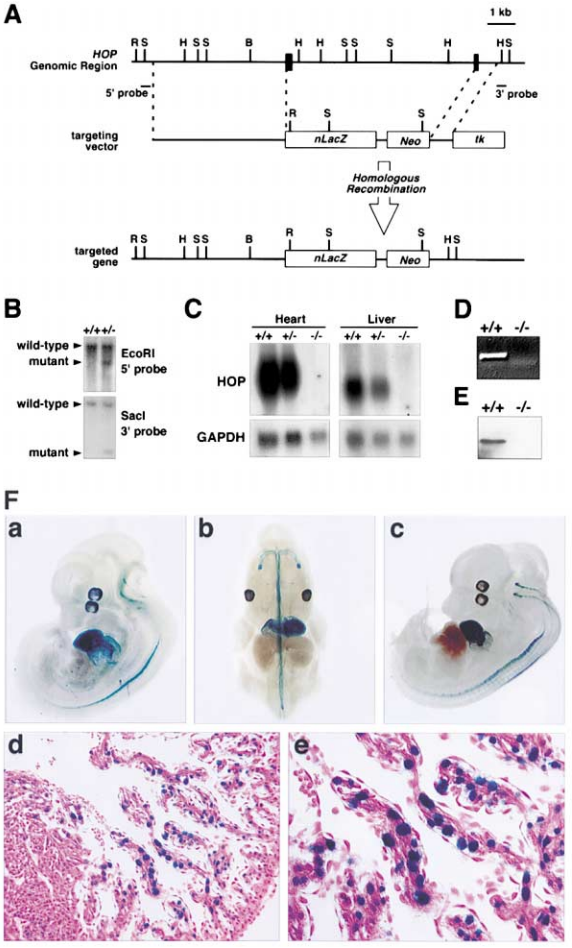

Figure 3. Generation of *HOP* Mutant Mice

(A) Strategy for targeting the mouse *HOP* gene by homologous recombination.

(B) Southern blot analysis of genomic DNA from a wild-type and $HOP^{+/-}$ mouse.

(C) Detection of *HOP* transcripts by Northern blot analysis.

(D) Detection of *HOP* transcripts by RT-PCR.

(E) Detection of HOP protein by Western blot analysis. The HOP protein of 9 kDa was detected in heart from wild-type but not from homozygous mutant mice.

(F) Expression of lacZ from the targeted *HOP* allele. (a) E11.5, (b and c) E12.5, (d and e) H and E sections of the heart of an E11.5 embryo at low (d) and high (e) magnification. Nuclear lacZ staining is largely confined to the trabecular region.

mutation eliminated expression of *HOP* mRNA (Figures 3C and 3D). Western blot analysis from brain and heart of *HOP* null mice also showed that the HOP protein of ~9 kDa was absent in homozygous mutants (Figure 3E and data not shown).

LacZ Expression from the Targeted *HOP* Allele

Embryos harboring the *HOP* mutation expressed lacZ in a pattern corresponding to that of the endogenous *HOP* gene (Figure 3F). Cardiac expression of lacZ was especially prominent after E10.5 (Figure 3F, a–c). Serial sections of the heart at E11.5 revealed the highest levels of lacZ staining within cardiomyocyte nuclei in the trabecular zone, where proliferation is diminished relative to the adjacent compact zone in the ventricular wall (Figure 3F, d and e). LacZ staining was also observed within the neural tube (Figure 3F, b).

Table 1. Genotypes of Offspring from $HOP^{-/-}$ Intercrosses

Genetic Background	Offspring of Each Genotype		
	+/+	+/−	−/−
129	32 (25%)	74 (58%)	22 (17%)
129/BL6	30 (21%)	83 (56%)	34 (23%)

Genotypes of mice from $HOP^{+/-}$ intercrosses were determined at P10. Absolute numbers of mice of each genotype are shown and the percent of total is in parentheses. In the isogenic 129Sv background, homozygous *HOP* mutants represented 17% of offspring at P10, which is lower than expected from Mendelian ratios ($p < 0.05$). In the mixed 129Sv/BL6 background, the frequency of homozygous *HOP* mutants was not statistically different from Mendelian ratios.

Embryonic Cardiac Defects in *HOP* Mutant Mice

In light of the lower than predicted number of viable *HOP* mutant mice in the isogenic 129Sv background, we examined embryos from timed pregnancies of $HOP^{+/-}$ intercrosses for possible lethal defects. We did not detect abnormal embryos prior to E9.5. However, at E11.5, approximately 10% of embryos showed arrested development (Figure 4, compare A and B). Genotyping confirmed that these were homozygous mutants. The hearts from these embryos did not show gross morphologic abnormalities, but the ventricular myocardium was extremely thin and hypocellular (Figure 4, compare C and E with D and F). There were also numerous ruptures throughout the ventricular walls, and there was a bloody pericardium. These findings suggest that *HOP* is required in a relatively small subset of isogenic embryos to establish the appropriate number of cardiac myocytes needed for the heart to sustain hemodynamic load beyond E11.5.

Cardiomyocyte Hyperplasia in *HOP* Mutant Mice

Since the majority of *HOP* mutants were viable, we analyzed them for possible cardiac abnormalities after birth. Viable *HOP* mutant mice in the isogenic 129Sv and mixed genetic backgrounds had hearts with increased ventricular wall thickness compared to control littermates (Figure 5A). At P1, the heart weight/body weight ratio in mutant mice was approximately 20% higher than in wild-type littermates. This increase in relative cardiac size was maintained until adulthood (Figure 5B).

Histologic examination and DAPI staining of mutant hearts suggested that the increase in size at early ages was largely due to an increase in cardiomyocyte cell number rather than hypertrophy (Figure 5A). This was confirmed by dissociating hearts from wild-type and mutant littermates and performing cell counts that distinguished cardiac myocytes from fibroblasts. As shown in Figure 5C, there was approximately a 30% increase in the number of cardiac myocytes in mutant hearts at P1 and P28. The size of cardiomyocytes was similar in mutant and wild-type mice up to 4 weeks of age.

At six months of age, a subset of mutant mice developed severely enlarged and dilated hearts with fibrosis (Figure 5D). Histological analysis revealed that myocytes

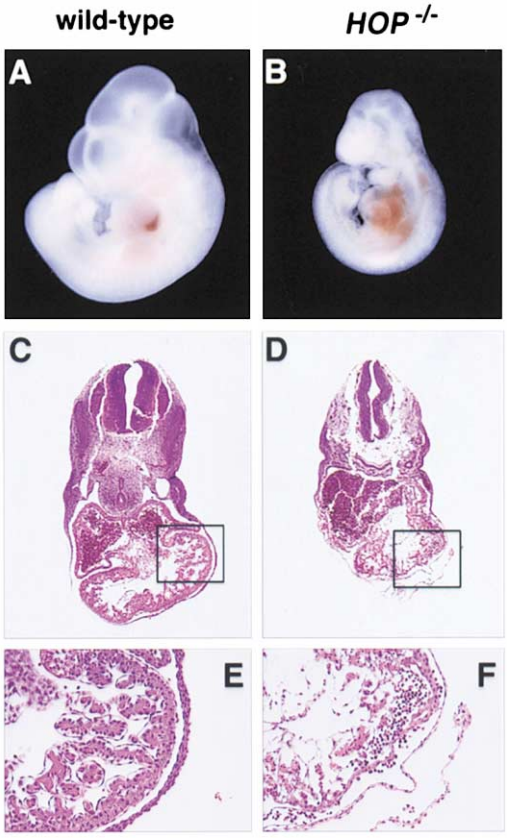

Figure 4. Abnormalities in Cardiac Development in *HOP* Mutant Mice

(A and B) Wild-type and HOP mutant embryos at E11.5. The *HOP* mutant shows abnormal cardiac morphology and pericardial hemorrhaging.

(C and D) H and E sections of wild-type and *HOP* mutant embryos at E11.5.

(E and F) The boxed regions in (C) and (D). Note the thin-walled myocardium in the mutant.

in these hearts were hypertrophic. Echocardiography of *HOP* mutant mice did not detect abnormalities in cardiac contractility or function, except in the subset of mutants that developed late-onset hypertrophy (data not shown).

Delayed Withdrawal of *HOP* Mutant Cells from the Cell Cycle

Cardiac muscle cells normally begin to withdraw from the cell cycle at birth. To determine whether the increase in cardiomyocyte cell number in *HOP* mutants was associated with prolonged proliferation, we stained histological sections of P1 hearts with antibody against phospho-histone H3, a marker of mitosis. Whereas phospho-H3-positive cells were observed only occasionally in wild-type hearts, they were widespread in the mutant hearts (Figure 5E). There were 19-fold more phospho-H3-positive cells in mutant than wild-type hearts. No phospho-H3-positive cardiomyocytes were detected in mutant or wild-type littermates at 4 weeks of age (data not shown), suggesting that cardiomyocyte proliferation was prolonged only during the neonatal period in the mutant. Increased cardiomyocyte cell numbers were observed in at least two-thirds of mutant mice, but there was variability in cell number.

Altered Gene Expression in Hearts from *HOP* Mutant Mice

In an effort to identify possible molecular defects in *HOP* mutant cardiomyocytes, we compared the gene expression profiles of wild-type and mutant hearts at P1 by microarray analysis (Table 2). According to our selection criteria for signal strength, background, expression ratio, and reproducibility, a total of 179 genes showed elevated expression and 90 showed reduced expression in mutants compared to controls. Numerous genes involved in cell proliferation were upregulated in mutant hearts. These included genes encoding cyclin D3 and basic transcription element binding protein 1(BTEB1) (Zhang et al., 2001a). *HOP* mutants also showed elevated expression of fetal genes that are typically associated with a cardiac stress response, including those encoding β-MHC, atrial natriuretic factor (ANF), b-type natriuretic factor (BNP), and skeletal α-actin. Interestingly, several smooth muscle-restricted genes, including those encoding SM22, calponin, smooth muscle α-actin, α-actinin-2, and cysteine-rich protein-2 (CRP2) were upregulated in mutant hearts. The changes in expression of several of the above genes were confirmed by RT-PCR analysis (Figure 6A).

Interference with SRF Activity by HOP

A striking number of the genes that were upregulated in the *HOP* mutant hearts were known targets for SRF (Table 2). We therefore tested whether HOP affected the activity of the *ANF*, *α-cardiac actin*, and *SM22* promoters, which contain essential SRF binding sites. HOP alone had no effect on these promoters, but it reduced the level of promoter activity in the presence of SRF (Figure 6B). SRF has been shown to interact with Nkx2.5 and GATA4, resulting in synergistic activation of the *ANF* and *cardiac α-actin* promoters (Chen and Schwartz, 1996). This synergy was suppressed by HOP in a dose-dependent manner (Figure 6B).

SRF also synergizes with the cardiac transcriptional cofactor, myocardin, which interacts with the MADS box of SRF (Wang et al., 2001). HOP diminished the responsiveness of the *SM22* and *ANF* promoters to myocardin (Figure 6B). The inhibitory effects of HOP on SRF activity were dose-dependent, but incomplete. Typically, we observed up to 50% inhibition of SRF activity in the presence of HOP. Higher amounts of HOP expression plasmid did not result in greater inhibition.

To begin to determine the mechanism whereby HOP repressed SRF-dependent gene transcription, we performed gel mobility shift assays with SRF and HOP proteins translated in vitro and a radiolabeled SRF binding site as a probe. HOP alone showed no detectable DNA binding and it diminished the binding of SRF in a dose-dependent manner (Figure 6C).

We tested whether ^{35}S-methionine-labeled HOP protein translated in vitro could associate with a GST-SRF fusion protein. Association of ^{35}S-methionine-labeled HOP with GST-SRF was readily detected in this assay, whereas no interaction of labeled HOP with GST alone was observed (Figure 6D). Immunoprecipitation assays

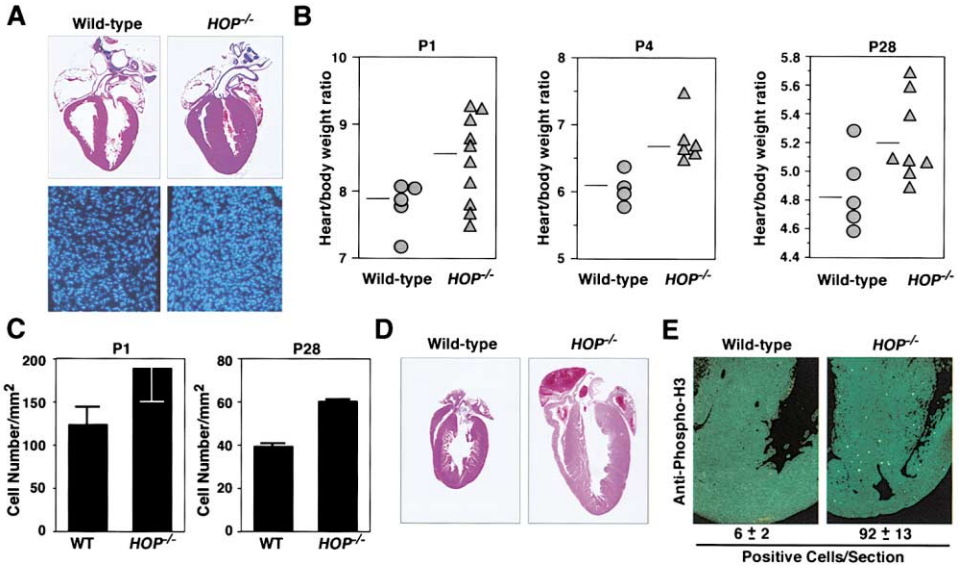

Figure 5. Cardiomyocyte Hyperplasia in *HOP* Mutant Mice

(A) Hearts from wild-type and *HOP* mutant mice at P1 were sectioned and analyzed by H and E staining (top). The lower images show DAPI staining of sections from the interventricular septum of wild-type and *HOP* mutant hearts.

(B) Heart weight/body weight ratios of wild-type and *HOP* mutant mice were determined at the indicated postnatal days. The bars indicate the average ratios for each group. Statistical significance of differences between wild-type and $HOP^{-/-}$ at each day were as follows: P1, $p < 0.02$; P4, $p < 0.005$; P28, $p < 0.05$.

(C) Hearts from wild-type and *HOP* mutant mice were dissociated and cardiomyocyte numbers were determined. Values represent the number of cells in a 1 mm^2 chamber. Cardiomyocytes were distinguished from fibroblasts by size and the presence of sarcomeres. $P < 0.01$ versus wild-type.

(D) Histological sections of hearts from wild-type and *HOP* mutants at six months of age. The mutant heart is hypertrophic.

(E) Representative histological sections from wild-type and *HOP* mutant hearts were stained with anti-phospho-histone H3 antibody. The number of positive cells from five different hearts of each genotype was quantified and is shown beneath each image.

Table 2. Genes Upregulated in *HOP* Mutant Hearts

Genes	Increase in Expression	SRF Target
Growth-associated genes		
Cyclin D3	3x	?
BTEB1/Kruppel-like factor	5x	?
Early growth factor response gene	3x	yes
Homer immediate early gene	3x	?
Defender Against Death (DAD1)	3x	?
Smooth muscle genes		
SM22	2x	yes
Calponin	3x	yes
Smooth muscle alpha-actin	2x	yes
Alpha-actinin-2	3x	?
Cysteine-rich protein-2	3x	yes
Cardiac muscle genes		
ANF	5x	yes
BNP	5x	?
SERCA	3x	yes
Skeletal alpha-actin	2x	yes
Beta-MHC	15x	yes
Cardiac MLC	3x	yes
Myosin binding protein-C	10x	?

Selected genes that were upregulated in *HOP* mutant hearts at P1 are shown. Relative increases in expression from microarray analysis are shown. Most changes were confirmed by RT-PCR analysis. Genes that are known to regulated by SRF in previous studies are indicated "yes" and genes not shown to be regulated by SRF are indicated "?".

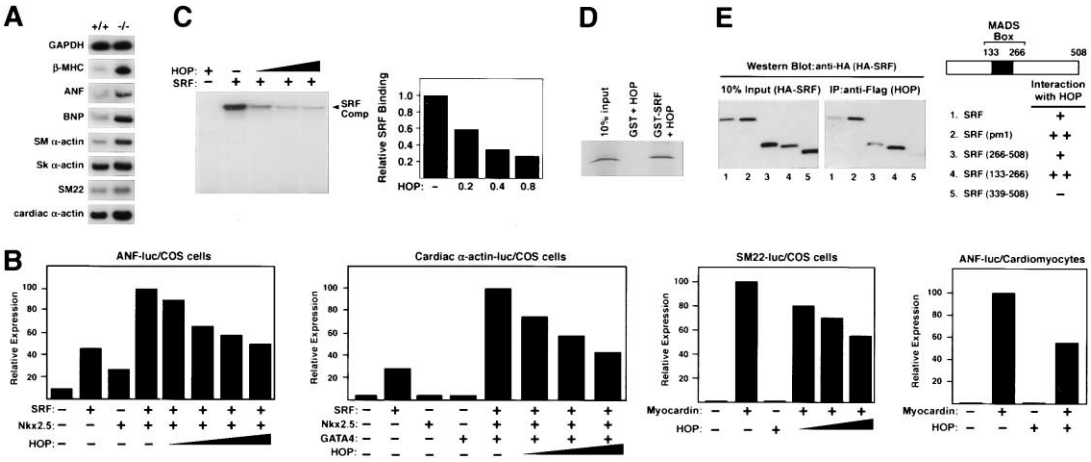

Figure 6. Changes in Gene Expression in Hearts from *HOP* Mutant Mice and Modulation of SRF Activity by HOP

(A) RT-PCR analysis of selected genes in P1 hearts of wild-type and *HOP* mutant mice.

(B) COS-1 cells (left three images) or cardiomyocytes (right image) were transiently transfected with the indicated luciferase reporters and expression vectors encoding HOP, SRF, Nkx2.5, GATA4, and myocardin, as described in Experimental Procedures. Values are expressed as relative luciferase activity compared to the maximum level. Representative experiments are shown. All assays were performed at least three times with comparable results.

(C) SRF and increasing amounts of HOP were translated in vitro and used in gel shift assays with a radiolabeled probe corresponding to the c-*fos* CArG box. Parallel translation reactions containing [^{35}S]-methionine were used to quantify relative amounts of translated proteins (not shown).

(D) GST-pull down assays. ^{35}S-methionine-labeled HOP protein was incubated with GST or GST-SRF, followed by binding to glutathione-agarose beads. Labeled proteins were resolved by SDS-PAGE. One-tenth of ^{35}S-methionine-labeled HOP protein used in GST-SRF pull-down assays was loaded in the input lane.

(E) Coimmunoprecipitation of Flag-tagged HOP and HA-tagged SRF from transiently transfected 293T cells. Immunoprecipitations were carried out with agarose-conjugated anti-Flag antibody. Immunoprecipitates were separated by SDS-PAGE and subsequently immunoblotted with anti-HA antibody (right image). One-tenth of the cell extract was immunoblotted with anti-HA antibody as input (left image).

from 293T cells cotransfected with expression plasmids encoding Flag-tagged HOP and HA-tagged SRF proteins also revealed an interaction between HOP and SRF. Using a series of SRF deletion mutants, we found that the MADS box of SRF mediated interaction with HOP (Figure 6E). A weaker, but still significant, interaction was also observed between HOP and the C-terminal region (residues 266–508) of SRF. An SRF mutant that cannot bind DNA (mutant pm1, Chen and Schwartz, 1996) was also able to interact with HOP.

Discussion

HOP is an unusual homeodomain protein that modulates cardiac growth and development. The phenotypes of *HOP* mutant mice suggest that HOP acts at two stages of heart development; prior to E11.5, it is involved in expansion of the ventricular myocardium, and later in fetal development it restricts cardiomyocyte proliferation. The effects of HOP on the developing heart correlate with its action as an antagonist of SRF, which plays a dual role in regulating gene expression during cell growth and muscle cell differentiation (Figure 7).

Negative Regulation of SRF Activity by HOP

The properties of HOP are reminiscent of those of I-POU, a member of the POU-homeodomain family that cannot bind DNA and inhibits the activity of other POU-domain transcription factors by forming inactive heterodimeric complexes (Treacy et al., 1991). This type of inhibitory activity is also analogous to that of the helix-loop-helix (HLH) protein Id, which lacks a DNA binding domain and forms inactive heterodimers with basic HLH proteins (Benezra et al., 1990). In light of the ability of homeodomain proteins to associate with HLH and GATA transcription factors (Lee et al., 1998; Sun et al., 2001), which play key roles in cardiac development (Srivastava and Olson, 2000), it will be of interest to determine whether HOP has additional positive or negative partners in the cardiac lineage.

A variety of homeodomain proteins have been shown to associate with SRF, but HOP is unique in its antago-

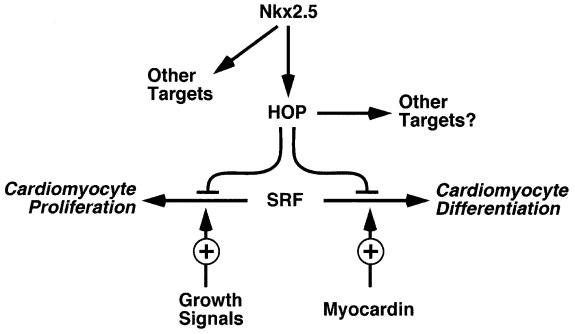

Figure 7. A Model for the Modulation of SRF Activity by HOP

SRF regulates the opposing processes of cell proliferation and differentiation. HOP antagonizes the activity of SRF. In the absence of HOP, the balance between proliferation and differentiation is disrupted with resulting excess or deficiency of cardiomyocytes, depending on other factors and signals.

nism of SRF DNA binding. The homeodomain protein prx1 enhances SRF activity by increasing the on-rate for DNA binding (Grueneberg et al., 1992). Nkx2.5 also binds DNA cooperatively with SRF, resulting in synergistic activation of SRF-dependent cardiac target genes (Chen and Schwartz, 1996; Sepulveda et al., 2002). Likewise, the Barx2 homeodomain protein associates with SRF and stimulates DNA binding, although the physiologic significance of this interaction has not been determined (Herring et al., 2001). HOP could interfere with SRF DNA binding by interference with critical contacts between residues that make essential base contacts or by disrupting SRF dimerization.

Previous studies of other homeodomains have demonstrated that helices 1 and 2, which form a virtually continuous surface oriented away from the DNA binding site, mediate protein-protein interactions (Wilson et al., 1995). Within this region, position 22 is critical in determining the specificity of such interactions. Homologies among the SRF-interacting homeodomains of HOP, Nkx2.5, prx1, and Barx2 are shown in Figure 1B. There are apparent identities among these homeodomains, but they are divergent at position 22, suggesting that additional determinants mediate their association with SRF. In this regard, at least two separable subdomains of the Nkx2.5 homeodomain have been shown to mediate association with SRF (Chen and Schwartz, 1996).

SRF recruits myocardin, which is expressed specifically in cardiac and smooth muscle cell lineages, to activate transcription through the CArG box (Wang et al., 2001). Our results show that HOP can diminish the cooperativity between SRF and myocardin. We presume this reflects the inhibition of SRF DNA binding by HOP, but it is also possible that HOP and myocardin compete for interaction with SRF.

Regulation of HOP Expression in the Developing Heart

The loss of *HOP* expression in *Nkx2.5* mutant embryos suggests that *Nkx2.5* acts upstream of *HOP* in a cascade of cardiogenic regulators. Consistent with this notion, we have identified a 1.2 kb cardiac enhancer upstream of *HOP* that contains multiple Nkx2.5 binding sites (data not shown).

The process of cardiac development is exquisitely sensitive to the level of Nkx2.5 expression and activity. Haploinsufficiency of Nkx2.5 expression in mice and humans results in cardiac structural abnormalities and conduction defects (Schott et al., 1998). Conversely, overexpression of Nkx2.5 in transgenic mice results in embryonic lethality due to abnormal cardiac morphogenesis (Kasahara et al., 2001). Overexpression of Nkx2.5 in frog and zebrafish embryos also results in expansion of the cardiac field with resulting enlargement of the heart (Chen and Fishman, 1996; Cleaver et al., 1996). Thus, mechanisms must exist to precisely govern Nkx2.5 activity during development. HOP acts indirectly to modulate Nkx2.5 activity by suppressing the activity of SRF, a key cardiogenic cofactor for Nkx2.5.

Regulating the Balance of Cardiac Growth and Differentiation

Prior to E11.5, HOP is expressed throughout the developing myocardium. However, after this point, HOP expression becomes restricted to the trabecular region, where the proliferative rate of cardiomyocytes is diminished relative to the adjacent compact zone (Pasumarthi and Field, 2002). Embryonic day 11.5 appears to represent a critical stage in heart development with respect to HOP activity, since a subset of *HOP* mutant embryos dies at this stage from cardiac insufficiency. The abnormalities in these mutant embryos appear to be cellular rather than morphologic, as looping morphogenesis and atrioventricular chamber formation occurs normally, but affected embryos have fewer cardiomyocytes and a thin-walled myocardium.

Mutant embryos that can survive past E11.5 progress to birth and show an excess of cardiomyocytes. This phenotype seems to result from prolonged proliferation of cardiomyocytes. However, this proliferative phenotype is transient, and mutant myocytes ultimately exit the cell cycle. It is intriguing that these mutant embryos exhibit a hypercellular cardiac phenotype, seemingly opposite to that of embryos that die at E11.5. How can the antithetical phenotypes of the two classes of *HOP* mutants be explained? One possibility is that they reflect the dual functions of SRF as a regulator of muscle cell proliferation and differentiation and the role of HOP in modulating SRF activity (Figure 7). Early in development when the myocardium must rapidly expand to sustain hemodynamic output, HOP may be required to dampen the differentiation-inducing activity of SRF, thereby favoring proliferation of cardiomyocytes. Conversely, at later stages, HOP may negatively regulate the growth-promoting function of SRF thereby promoting terminal differentiation. Based on the ability of HOP to diminish SRF activity, the absence of HOP would be predicted to result in either precocious withdrawal of myocytes from the cell cycle or a failure of myocytes to differentiate properly. We also cannot exclude the possibility that HOP has targets in addition to SRF that contribute to the mutant phenotype.

The dual roles of SRF in cell proliferation and muscle cell differentiation are well established (Poser et al., 2000; Vandromme et al., 1992; Croissant et al., 1996). SRF binds CArG box sequences in the control regions of growth-regulated and muscle-specific genes (reviewed in Reecy et al., 1998). Consistent with the notion that SRF activity is augmented in the absence of HOP, numerous CArG box-dependent genes were upregulated in *HOP* mutant hearts. Studies in skeletal muscle cells that express SRF antisense RNA under control of a steroid-inducible promoter have demonstrated that relatively minor changes in SRF activity can differentially affect cell proliferation or differentiation (Soulez et al., 1996). At intermediate levels of SRF antisense RNA expression, cells were able to proliferate, but not differentiate, whereas further elevation of SRF antisense expression blocked proliferation. The ability of SRF to regulate the opposing processes of proliferation and muscle cell differentiation is dependent on its association with positive and negative cofactors and on intracellular signaling and is consistent with the antithetical cardiac phenotypes of *HOP* mutant mice.

In skeletal and smooth muscle cells, proliferation and differentiation are mutually exclusive processes. In contrast, cardiac myocytes can divide and differentiate simultaneously during early development, but terminal

differentiation of cardiomyocytes is associated with irreversible cell cycle exit. The segregation of *HOP* mutants into two distinct classes with opposite phenotypes suggests that HOP participates in a very finely tuned mechanism that governs the balance between cardiomyocyte proliferation and differentiation. While HOP acts as a negative modulator of SRF, it does not completely repress SRF activity. This partial effect of HOP on SRF activity may explain why *HOP* mutants segregate into two classes rather than showing a single phenotype. The variable penetrance of *HOP* mutant phenotypes also suggests the existence of modifier genes that influence the activity of SRF, which is not surprising given the plethora of cofactors and signaling pathways that modulate SRF activity.

While we favor the interpretation that HOP exerts its effects on cardiomyocytes in a cell-autonomous manner, it is formally possible that HOP also has effects on other cell types that influence cardiac growth and development. It is notable in this regard that other thin-walled myocardial phenotypes have been attributed to defects in non-cardiac tissues (Wu et al., 1999). Thus far, we have not detected defects in other tissues in which HOP is expressed, such as the liver and lung, in mutant mice.

Implications for Congenital and Acquired Cardiac Disease

In addition to its role in myoblast proliferation and differentiation, SRF is a target for a variety of stress-inducible signaling pathways and has been implicated in reprogramming cardiac gene expression in response to hypertrophic signals. Overexpression of SRF under control of a cardiac promoter has recently been shown to result in hypertrophic growth of the heart (Zhang et al., 2001b). This is consistent with the phenotype of the subset of *HOP* mutants, which show late-onset hypertrophy. In light of the pivotal role of SRF in myocyte growth and differentiation, it will be interesting to examine the potential involvement of HOP in acquired and congenital forms of heart disease.

Experimental Procedures

Cloning and Sequencing of HOP

In order to identify novel heart-enriched homeodomain proteins, EST databases were screened using a consensus sequence for the homeodomain. EST AA222563, which encodes HOP, was isolated from a 6-week-old mouse heart cDNA library. Full-length cDNA clones were obtained by 5′ rapid amplification of cDNA ends (RACE) and by screening a mouse heart cDNA library (Stratagene) with the EST as a probe.

RNA and In Situ Hybridization Analysis

A mouse multiple tissue Northern blot (Clontech) was hybridized under high stringency conditions with a ^{32}P-labeled probe prepared from EST A222563 to detect HOP transcripts in adult tissues. In situ hybridization of whole embryos or paraffin sections was performed as described (Passier et al., 2000). Identical bright and dark field images were captured and silver grains were pseudo-colored red using Adobe Photoshop, after which images were superimposed.

Generation of *HOP* Mutant Mice

The *HOP* targeting vector was constructed in a plasmid containing nuclear LacZ (nLacZ), PolNeo, and HSV-TK cassettes. SM-1 ES cells derived from a 129/SvEv mouse strain were electroporated with the targeting vector and doubly selected in G418 and FIAU. ES clones were picked and homologous recombination was confirmed by Southern analysis. Recombinant ES cell clones were injected into blastocysts obtained from C57BL6/J females. Chimeras were mated with C57BL6/J females to obtain F1 mice carrying the targeted allele. Mice were generated in the isogenic 129/Sv background by breeding the chimeras with 129/Sv females.

Immunohistochemistry

Histological sectioning and staining with hematoxylin/eosin were performed according to standard techniques. For immunostaining, sections were deparaffinized in xylene, rehydrated through graded ethanols to PBS, and permeabilized in 0.3% Triton X-100 in PBS. Nonspecific binding was blocked by 1.5% normal goat serum in PBS and anti-phospho-histone H3 rabbit antibody (Upstate Biotechnology) was applied at a 1:200 dilution in 0.1% BSA in PBS overnight at 4°C. Sections were washed in PBS and fluorescein-conjugated anti-rabbit antibody (Vector Laboratories) was applied at a 1:200 dilution in 1% normal goat serum for 1 hr.

Quantification of Cardiomyocyte Cell Numbers

Cardiomyocytes from neonatal and adult hearts were isolated using an alkaline dissociation method (Tamura et al., 1998) with minor modifications. In brief, hearts were dissected, placed in 10% neutral-buffered formalin, and fixed at 4°C. Hearts were then treated with 50% KOH overnight at 4°C, followed by extensive washing in distilled water. Specimens were dried before addition of PBS containing Hoechst 33342 to yield a final suspension of ~10 mg fixed tissue/ml. Cell suspension was diluted with an equal volume of PBS and 18 μl were loaded onto a Fuchs-Rosenthal counting chamber (Hausser Scientific). Cardiomyocytes in the counting chamber were distinguished from fibroblasts by cytoplasmic size and phase contrast microscopy. The total number of cardiomyocytes from each individual heart was calculated using the following equation:

Cell number = 5000 × number of cells/mm^2 counting chamber × dilution factor × total volume. The total numbers of cardiomyocytes from wild-type neonatal hearts using this method were in the range of 10^6, which is similar to reported values using other methods (Reiss et al., 1996; Liao et al., 2001).

Microarray Analysis

RNA was extracted from wild-type and mutant hearts using Trizol reagent (Gibco BRL). For each group, 3 hearts were pooled and microarray analysis was performed twice. One hundred ng of total RNA was amplified using the Atlas SMART Probe Amplification Kit (Clontech). The optimum number of PCR amplification cycles was determined following the manufacturer's instructions. After the generation of cDNA, 3 amplification reactions were subjected to 19 cycles of PCR using a MWG Primus HT thermocycler. The 3 reactions were pooled and unreacted PCR primers and dNTP's were removed using a QIAquick PCR purification kit (Qiagen). Amplified cDNA was labeled using a modification of the Bioprime DNA labeling kit (Invitrogen). It was then added to a microarray containing 27,648 murine cDNA elements and incubated at 50°C for 18–24 hr. The arrays were washed, scanned on an Axon GenePix 4000, and the signal intensities for each element were determined using Gene Pix Pro (Axon) as described (Wei et al., 2002).

Microarray analysis was performed in duplicate, reversing the Cy-Dyes. The data was preprocessed with an intensity dependent normalization factor (Yang et al., 2002) derived from the Lowess function contained in the R statistical package. After the preprocessing, the data was imported into a custom Access database and queried for an expression log ratio of greater than 1 or less than −1, reproducibility in dye swap arrays, and a minimum median signal intensity of twice local background.

Glutathione S-Transferase Pull-Down Assays

A cDNA encoding the complete 508 amino acid human SRF protein was cloned in-frame to Glutathione-S-Transferase (GST) in the pGEX-KG vector. GST-SRF fusion protein was expressed and purified as described (Guan and Dixon, 1991). HOP protein was translated in a rabbit reticulocyte lysate (Promega) supplemented with [^{35}S]-methionine. For GST-pull-down assays, equal amounts of GST-

SRF or GST (as negative control) were incubated with 10 μl of ^{35}S-labeled HOP in 250 μl GST binding buffer (PBS with 0.5% NP-40 and 5 mM EDTA) for 2 hr at 4°C. After washing with GST binding buffer, proteins associated with GST-agarose beads were analyzed with 4%–20% SDS-PAGE and visualized by autoradiography. One μl of in vitro translated ^{35}S-labeled HOP was loaded as input control.

Immunoprecipitation and Western Blot Analysis

Expression vectors encoding Flag-tagged HOP and HA-tagged SRF were transfected into 293T cells. Cells were harvested 30 hr later and lysed in 1 ml of ice-cold PBS supplemented with complete protease inhibitors (Roche), 0.5% Triton X-100, 1 mM EDTA, and 40 units of DNAase I (Roche Molecular Biochemicals). Immunoprecipitations were carried out by incubating 500 μl lysate with 20 μl FLAG-sepharose (Sigma) at 4°C for 3 hr. The beads were washed twice with lysis buffer and boiled in SDS sample buffer. Immunoprecipitated proteins were analyzed by Western blotting using rat anti-HA antibody. Anti-HOP antibody was generated by Cocalico Biologicals (Reamstown, PA) using GST-HOP.

Gel Mobility Shift Assays

SRF (0.2 μg cDNA) was transcribed and translated in vitro in the presence of increasing amounts of HOP (0.2, 0.4, and 0.8 μg cDNA) in 25 μl total volume with a TNT T7-coupled reticulocyte lysate system supplemented with [^{35}S]-methionine. Gel mobility shift assays were performed with ^{32}P-labeled oligonucleotides corresponding to the sequence of the c-*fos* SRE as described (Chang et al., 2001). The amount of shifted probe was quantified with a phosphoimager and normalized against the amount of translated ^{35}S-labeled SRF protein in each binding reaction.

Transfection Assays

The ANF-luciferase construct contained the 2.6 kb promoter (Hiroi et al., 2001). The cardiac α-actin promoter-luciferase construct contained the 0.3 kb avian promoter (Chen and Schwartz, 1996). The SM22-luciferase construct contained the 1434 bp promoter (Li et al., 1997). N-terminal HA-tagged human SRF and SRF deletion mutants were cloned into the pCGN expression vector, which contains the CMV promoter (Chen and Schwartz, 1996). N-terminal FLAG-tagged HOP was cloned into pcDNA3.1 (Invitrogen). The pcDNA-myocardin vector was described previously (Wang et al., 2001).

COS cells were maintained in Dulbecco's Minimal Essential Medium with 10% fetal bovine serum. Primary neonatal rat cardiomyocytes were prepared as described (Molkentin et al., 1998). COS cells were transfected using FuGENE 6 reagent (Roche) with 0.2 μg of reporter and expression constructs. Neonatal cardiomyocytes were transfected using Lipofectamine plus (Gibco BRL) with 0.2 μg luciferase reporters, 0.2 μg myocardin, and 0.5 μg HOP expression plasmids. Fifty ng of a CMV-lacZ reporter was included as an internal control for transfection efficiency. In titration experiments with HOP, between 0.1 and 0.8 micrograms of HOP expression plasmid were used. The pcDNA3.1 vector without a cDNA insert was used to equalize the amount of DNA in each transfection. Cell extracts were prepared 36 hr after transfection and assayed for luciferase activity using the Promega Luciferase detection kit. Luciferase activities were normalized to β-galactosidase activity. Each experiment was performed in duplicate. Transfection assays were performed at least 3 times with comparable results.

Acknowledgments

We thank Jon Epstein for sharing results prior to publication, Richard Harvey for Nkx2.5 mutant mice, and Robert Schwartz, Yukio Hiroi, and Issei Komuro for reagents. We are grateful to Deepak Srivastava for comments on the paper, Norbert Frey for echocardiography Yin-Chai Cheals for blastocyst injections, and John Shelton for his assistance with fluorescence microscopy. Supported by grants from NIH, The D.W. Reynolds Center for Clinical Cardiovascular Research, and the McGowan Charitable Fund to E.N.O.

Received: July 8, 2002
Revised: August 7, 2002

References

Benezra, R., Davis, R., Lockshon, D., Turner, L., and Weintraub, H. (1990). The protein Id: a negative regulator of helix-loop-helix DNA binding proteins. Cell *61*, 49–59.

Chang, P.S., Li, L., McAnally, J., and Olson, E.N. (2001). Muscle specificity encoded by specific serum response factor-binding sites. J. Biol. Chem. *276*, 17206–17212.

Chen, C.Y., and Schwartz, R.J. (1996). Recruitment of the tinman homolog Nkx-2.5 by serum response factor activates cardiac α-actin gene transcription. Mol. Cell. Biol. *16*, 6372–6384.

Chen, J., and Fishman, M. (1996). Zebrafish tinman homolog demarcates the heart field and initiates myocardial differentiation. Development *122*, 3809–3816.

Chen, F., Kook, H., Milewski, R., Gitler, A.D., Lu, M.M., Li, J., Nazarian, R., Schnepp, R., Kuangyu, J., Biben, C., et al. (2002). *Hop* is an unusual homeobox gene that modulates cardiac development. Cell *110*, this issue, 713–723.

Cleaver, O., Patterson, K., and Krieg, P. (1996). Overexpression of the tinman-related genes XNkx2.5 and XNkx2.3 in *Xenopus* embryos results in myocardial hyperplasia. Development *122*, 3549–3556.

Croissant, J., Kim, J., Eichele, G., Goering, L., Lough, J., Prywes, R., and Schwartz, R. (1996). Avian serum response factor expression restricted primarily to muscle cell lineages is required for α-actin gene transcription. Dev. Biol. *177*, 250–264.

Guan, K.L., and Dixon, J.E. (1991). Eukaryotic proteins expressed in *Escherichia coli*: an improved thrombin cleavage and purification procedure of fusion proteins with glutathione S-transferase. Anal. Biochem. *192*, 262–267.

Gehring, W.J., Affolter, M., and Burglin, T. (1994). Homeodomain proteins. Annu. Rev. Biochem. *63*, 487–526.

Grueneberg, D.A., Natesan, S., Alexandre, C., and Gilman, M.Z. (1992). Human and *Drosophila* homeodomain proteins that enhance the DNA-binding activity of serum response factor. Science *257*, 1089–1095.

Harvey, R.P. (1996). NK-2 homeobox genes and heart development. Dev. Biol. *178*, 203–216.

Herring, B.P., Kriegel, A.M., and Hoggatt, A.M. (2001). Identification of Barx2b, a serum response factor-associated homeodomain protein. J. Biol. Chem. *276*, 14482–14489.

Hiroi, Y., Kudoh, S., Monzen, K., Ikeda, Y., Yazaki, Y., Nagai, R., and Komuro, I. (2001). Tbx5 associates with Nkx2–5 and synergistically promotes cardiomyocyte differentiation. Nat. Genet. *28*, 276–280.

Kasahara, H., Wakimoto, H., Liu, M., Maguire, C.T., Converso, K.L., Shioi, T., Huang, W.Y., Manning, W.J., Paul, D., Lawitts, J., et al. (2001). Progressive atrioventricular conduction defects and heart failure in mice expressing a mutant Csx/Nkx2.5 homeoprotein. J. Clin. Invest. *108*, 189–201.

Kornberg, T.B. (1993). Understanding the homeodomain. J. Biol. Chem. *268*, 26813–26816.

Lee, Y., Shioi, T., Kasahara, H., Jobe, S., Wiese, R., Markham, B., and Izumo, S. (1998). The cardiac tissue-restricted homeobox protein Csx/Nkx2.5 physically associates with the zinc finger protein GATA4 and cooperatively activates atrial natriuretic factor gene expression. Mol. Cell. Biol. *18*, 3120–3129.

Li, L., Liu, Z., Mercer, B., Overbeek, P., and Olson, E.N. (1997). Evidence for serum response factor-mediated regulatory networks governing SM22α transcription in smooth, skeletal, and cardiac muscle cells. Dev. Biol. *187*, 311–321.

Liao, H., Kang, P., Nagashima, H., Yamasaki, N., Usheva, A., Ding, B., Lorell, B., and Izumo, S. (2001). Cardiac-specific overexpression of cyclin-dependent kinase 2 increases smaller mononuclear cardiomyocytes. Circ. Res. *88*, 443–450.

Lin, Q., Schwarz, J., Bucana, C., and Olson, E.N. (1997). Control of mouse cardiac morphogenesis and myogenesis by transcription factor MEF2C. Science *276*, 1404–1407.

Lints, T., Parsons, L., Hartley, L., Lyons, I., and Harvey, R. (1993). Nkx2.5: a novel murine homeobox gene expressed in early heart progenitor cells and their myogenic descendants. Development *119*, 969.

Lyons, I., Parsons, L., Hartley, L., Li, R., Andrews, J., Robb, L., and Harvey, R. (1995). Myogenic and morphogenetic defects in the heart tubes of murine embryos lacking the homeobox gene Nkx2.5. Genes Dev. *9*, 1654–1666.

Molkentin, J.D., Lu, J.R., Antos, C.L., Markham, B., Richardson, J., Robbins, J., Grant, S.R., and Olson, E.N. (1998). A calcineurin-dependent transcriptional pathway for cardiac hypertrophy. Cell *93*, 215–228.

Norman, C., Runswick, M., Pollock, R., and Treisman, R. (1988). Isolation of properties of cDNA clones encoding SRF, a transcriptional factor that binds to the c-*fos* serum response element. Cell *55*, 989–1003.

Passier, R., Richardson, J.A., and Olson, E.N. (2000). Oracle, a novel PDZ-LIM domain protein expressed in heart and skeletal muscle. Mech. Dev. *92*, 277–284.

Pasumarthi, K.B.S., and Field, L.J. (2002). Cardiomyocyte cell cycle regulation. Circ. Res. *90*, 1044–1054.

Poser, S., Impey, S., Trinh, K., Xia, Z., and Storm, D. (2000). SRF-dependent gene expression is required for PI3-kinase-regulated cell proliferation. EMBO J. *19*, 4955–4966.

Reecy, J., Belaguli, N., and Schwartz, R. (1998). SRF/homeobox protein interactions. In Heart Development, R. Harvey and N. Rosenthal, eds. (San Diego, CA: Academic Press), pp 273–290.

Reiss, K., Cheng, W., Ferber, A., Kajstura, J., Li, P., Li, B., Olivetti, G., Homcy, C., Baserga, R., and Anversa, P. (1996). Overexpression of insulin-like growth factor-1 in the heart is coupled with myocyte proliferation in transgenic mice. Proc. Natl. Acad. Sci. USA *93*, 8630–8635.

Schott, J.J., Benson, D.W., Basson, C.T., Pease, W., Silberbach, G.M., Moak, J.P., Maron, B.J., Seidman, C.E., and Seidman, J.G. (1998). Congenital heart disease caused by mutations in the transcription factor NKX2–5. Science *281*, 108–111.

Sepulveda, J.L., Vlahopoulos, S., Iyer, D., Belaguli, N., and Schwartz, R.J. (2002). Combinatorial expression of GATA4, Nkx2–5 and serum response factor directs early cardiac gene activity. J. Biol. Chem. *277*, 25775–25782.

Smith, D., and Johnson, A. (1992). A molecular mechanism for combinatorial control in yeast: MCM1 protein sets the spacing and orientation of the homeodomains of an α 2 dimer. Cell *68*, 133–142.

Soulez, M., Rouviere, C., Chafey, P., Hentzen, D., Vandromme, M., Lautredou, N., Lamb, N., Kahn, A., and Tuil, D. (1996). Growth and differentiation of C2 myogenic cells are dependent on serum response factor. Mol. Cell. Biol. *16*, 6065–6074.

Srivastava, D., and Olson, E.N. (2000). A genetic blueprint for cardiac development. Nature *407*, 221–226.

Srivastava, D., Thomas, T., Lin, Q., Kirby, M.L., Brown, D., and Olson, E.N. (1997). Regulation of cardiac mesodermal and neural crest development by the bHLH transcription factor, dHAND. Nat. Genet. *16*, 154–160.

Sun, T., Echelard, Y., Lu, R., Yuk, D., Kaing, S., Stiles, C., and Rowitch, D. (2001). Olig bHLH proteins interact with homeodomain proteins to regulate cell fate acquisition in progenitors of the ventral neural tube. Curr. Biol. *11*, 1413–1420.

Tamura, T., Onodera, T., Said, S., and Gerdes, A.M. (1998). Correlation of myocyte lengthening to chamber dilation in the spontaneously hypersensitive heart failure (SHHF) rat. J. Mol. Cell. Cardiol. *30*, 2175–2181.

Tanaka, M., Chen, Z., Bartunkova, S., Yamasaki, N., and Izumo, S. (1999). The cardiac homeobox gene Csx/Nkx2.5 lies genetically upstream of multiple genes essential for heart development. Development *126*, 1269–1280.

Treacy, M.N., He, X., and Rosenfeld, M.G. (1991). I-POU: a POU-domain protein that inhibits neuron-specific gene activation. Nature *350*, 577–584.

Vandromme, M., Gauthier-Rouviere, C., Carnac, G., Lamb, N., and Fernandez, A. (1992). Serum response factor p67 SRF is expressed and required during myogenic differentiation of both mouse C2 and rat L6 muscle cell lines. J. Cell Biol. *118*, 1489–1500.

Wang, D., Chang, P.S., Wang, Z., Sutherland, L., Richardson, J.A., Small, E., Krieg, P.A., and Olson, E.N. (2001). Activation of cardiac gene expression by myocardin, a transcriptional cofactor for serum response factor. Cell *105*, 851–862.

Wei, Y., Harris, T.M., and Childs, G. (2002). Global gene expression patterns during neural differentiation of P19 embryonic carcinoma cells. Differentiation *70*, 204–219.

Wilson, D., Guenther, B., Desplan, C., and Kuriyan, J. (1995). High resolution crystal structure of a paired (pax) class cooperative homeodomain dimer on DNA. Cell *82*, 709–719.

Wu, H., Lee, S.H., Gao, J., Liu, X., and Iruela-Arispe, M.L. (1999). Inactivation of erythropoietin leads to defects in cardiac morphogenesis. Development *126*, 3597–3605.

Yang, Y.H., Dudoit, S., Luu, P., Lin, D.M., Peng, V., Ngai, J., and Speed, T.P. (2002). Normalization for cDNA microarray data: a robust composite method addressing single and multiple slide systematic variation. Nucleic Acids Res. *30*, e15.

Zhang, X., Azhar, G., Chai, J., Sheridan, P., Nagano, K., Brown, T., Yang, J., Khrapko, K., Borras, A.M., Lawitts, J., et al. (2001b). Cardiomyopathy in transgenic mice with cardiac-specific overexpression of serum response factor. Am. J. Physiol. Heart Circ. Physiol. *280*, H1782–H1792.

Zhang, X., Simmen, F., Michel, F., and Simmen, R. (2001a). Increased expression of the Zn-finger transcription factor BTEB1 in human endometrial cells is correlated with distinct cell phenotype, gene expression patterns, and proliferative responsiveness to serum and TGF-β1. Mol. Cell. Endocrinol. *181*, 81–96.

Accession Numbers

The GenBank accession number for the HOP cDNA sequences reported in this paper is AF534182.